

Ontology-Based Data Acquisition, Refinement, and Utilization in the Development of a Multilayer Ferrite Inductor

Björn Mieller,* Sahar Ben Hassine, Jörg Töpfer, Christoph Prieße, Arne Bochmann, Beate Capraro, Sebastian Stark, Uwe Partsch, and Carina Fresemann

A key aspect in the development of multilayer inductors is the magnetic permeability of the ferrite layers. Herein, the effects of different processing steps on the permeability of a NiCuZn ferrite are investigated. Dry-pressed, tape-cast, and cofired multilayer samples are analyzed. An automated data pipeline is applied to structure the acquired experimental data according to a domain ontology based on Platform MaterialDigital core ontology. Example queries to the ontology show how the determined process–property correlations are accessible to nonexperts and thus how suitable data for component design can be identified. It is demonstrated how the inductance of cofired multilayer inductors is reliably predicted by simulations if the appropriate input data corresponding to the manufacturing process is used.

community participates by contributing data is still a vision. A major challenge in creating such a data space is the highly interdisciplinary nature of this project. State-of-the-art approaches for semantic description and interoperable storage of data, web-based tools for authentication, and retrieval and processing of data must be combined with the specific knowledge of experts in the various MSE domains. Typically, however, MSE experts are not sufficiently trained in the development and use of the required digital tools. Although the various aspects of digitalization in MSE are widely presented and discussed, the concepts often remain very

1. Introduction


Digitalization in materials science and engineering (MSE) is currently a ubiquitous topic in the community. The motivation, the expected benefits, and the hurdles are comprehensively described in various perspective articles.^[1–5] The consensus is that a shared, well-organized materials data space offers many opportunities for accelerated and more efficient materials development. So far, a coherent material data space that is available to the entire MSE community and in which a large part of the

abstract for materials researchers and technologists. This means that the entry barriers for active participation in and further development of digitalization are comparatively high for many research groups and companies in MSE. There is a lack of practical examples that show how material properties, technological parameters, and simulation results can be found, accessed, inter-operably linked, stored, and used in a reproducible manner.

The MaterialDigital initiative (www.materialdigital.de) is working together with associated research projects to provide precisely such practical examples and thus create a basis for

B. Mieller
Division Advanced Multi-materials Processing
Department Materials Engineering
Bundesanstalt für Materialforschung und -prüfung (BAM)
Unter den Eichen 87, 12205 Berlin, Germany
E-mail: bjoern.mieller@bam.de

S. B. Hassine, C. Fresemann
Chair of Industrial Information Technology
Institute of Machine Tools and Factory Management
Technical University of Berlin
Pascalstr. 8-9, 10587 Berlin, Germany

 The ORCID identification number(s) for the author(s) of this article can be found under <https://doi.org/10.1002/adem.202401042>.

© 2024 The Author(s). Advanced Engineering Materials published by Wiley-VCH GmbH. This is an open access article under the terms of the Creative Commons Attribution License, which permits use, distribution and reproduction in any medium, provided the original work is properly cited.

DOI: 10.1002/adem.202401042

J. Töpfer, C. Prieße, A. Bochmann
Department of SciTec
Ernst-Abbe-Hochschule
University of Applied Sciences Jena
Carl-Zeiss-Promenade 2, 07745 Jena, Germany

B. Capraro
Department Hybrid Microsystems
Group Ceramic Tapes
Fraunhofer Institute for Ceramic Technologies and Systems IKTS
Michael-Faraday-Str.1, 07629 Hermsdorf, Germany

S. Stark
Department Smart Materials and Systems
Fraunhofer Institute for Ceramic Technologies and Systems IKTS
Winterbergstraße 28, 01277 Dresden, Germany

U. Partsch
Department Hybrid Microsystems
Fraunhofer Institute for Ceramic Technologies and Systems IKTS
Winterbergstraße 28, 01277 Dresden, Germany

the broad and low-threshold participation of the community in the creation of a material data space.

Here, we report on a corresponding example from the field of functional ceramic component development. The materials engineering task is to develop a multilayer ferrite inductor as a passive microelectronic component integrated in a multilayer low-temperature cofired ceramics (LTCC) architecture. Ceramic multilayer technology, cofiring of a dielectric base material with a new type of Ni–Cu–Zn ferrite as a magnetic functional material, is used. The fabrication depth ranges from the synthesis of various ferrite starting powders, to shaping by tape casting, and finally multilayer fabrication by structuring ceramic green tapes, stacking, laminating, and cofiring. The relationship between the particle size of the ferrite starting powder, the magnetic permeability of ferrite bulk samples and the inductance of the cofired multilayer coils is investigated. Along the process chain, selected material data and technological parameters are collected by domain experts and semantically linked using a domain ontology developed for this purpose. The application of the data linked in this way is demonstrated by example queries.

In this article, first the most important material science fundamentals and the current state of research on multilayer inductors are presented. Then, the fundamentals and concept of the ontology-based data processing and utilization are described. The results section is divided into three subsections. First, the material science results are presented. The second part describes the concrete implementation of data processing and semantic linking by an automated data pipeline. In the third part, querying the linked data is briefly demonstrated.

1.1. Ceramic Multilayer Technology

Multilayer technology is a special, very application-oriented ceramic fabrication route. The technology is well-established in the fields of passive multilayer components, including multilayer ceramic capacitors (MLCC),^[6] multilayer piezo actuators,^[7] and LTCC for electronic packaging.^[8,9] It comprises powder preparation, tape casting,^[10] structuring of tapes, stacking and lamination, cofiring, and post-processing. Powder synthesis includes mixing and milling of raw materials and sometimes dopants. Depending on the process route, a thermal treatment, calcination, is interposed to transform the raw materials mix into the desired chemical composition and crystallographic phase. Generally, many options for shaping of ceramic powders are possible, including dry-pressing, injection molding, additive manufacturing, slip casting, or tape casting. Each shaping technology requires a purposeful preparation of the powder with additives to create a granulate, feedstock, or slurry. The shaping technology determines the density of the powder compact, called green density, which in turn can strongly influence the sintering behavior. For tape casting, a slurry is prepared. In addition to the ceramic powder and a solvent, it contains organic binder, plasticizer, and further additives like dispersing agents. The slurry is cast onto a polymer substrate (Mylar tape) using a doctor-blade tape caster to give a flexible green tape after removing the solvent in a drying channel. The resulting green tape is a flexible polymer tape highly filled with ceramic particles, which can be structured using cutting and punching. Typically, metallization is realized

by screen printing of metal pastes. Vertical interconnects in the later multilayer (VIAs) are created by filling holes in the green tape with metal paste. Structured sections of the green tape, so-called green sheets, are then stacked and aligned to build up the intended multilayer. The stack is laminated by thermo-compression to fixate the alignment of the sheets. In the subsequent cofiring process, the organic binder is burned out and the powder compact densifies to form a monolithic ceramic microstructure. The metal paste is cofired simultaneously to give conductor paths or electrodes. Cofiring of the multilayer component is performed at temperatures below the melting temperature of the metal paste. This often requires lowering of the sintering temperature of the ceramic material by additives or adjusted compositions. Depending on the multilayer concept, specific post-processing steps like soldering and bonding of surface-mounted devices, polarization, or thin-film deposition may follow.

An essential common feature of all multilayer concepts is the combination of ceramics with other materials, or the combination of different ceramics, respectively. When combining or integrating different materials and material classes, mechanical misfits due to different shrinkage and thermal expansion as well as interface reactions must always be taken into account.^[11–14] The typical consequences of these effects are cracking, delamination, distortion, and changes in physical properties. So far, highly integrated multilayers and multi-material concepts can only be successfully realized on a large scale with closely specified material pairings or in individual case studies on a laboratory scale. These successful concepts are often based on a combination of domain-specific expertise and the experience of the technologists involved. The underlying development work is very complex due to the multistep technology and has so far only been transferable to product innovations to a limited extent. At the same time, new material variants are constantly being presented in the academic field, but these rarely make the transition from the laboratory to industrial utilization.

1.2. Cofiring of Ferrite and Multilayer Inductors

Cofired microelectronic ferrite components are an apt example of how difficult it is to commercialize multi-material multilayer concepts. The cofiring of low-sintering ferrite and dielectric base material has been researched for more than 10 years. The fabrication of cofired components on a laboratory scale has been demonstrated occasionally.^[15] Nevertheless, this technology has not yet been mastered and unexpected problems repeatedly arise in component development, as is also shown in this study.

An important group of soft magnetic materials used for many applications including power ferrites, electromagnetic interference devices, or multilayer inductors are NiCuZn ferrites.^[16,17] These ferrites are characterized by their low sintering temperature, high resistivity, medium permittivity, low losses, and excellent performance up to frequencies of up to several hundred MHz. Their magnetic properties depend, among other factors, on composition and microstructure. For applications as multilayer inductors, low sintering temperatures as low as 900 °C are required, because coil patterns are printed and fired using Ag metal pastes. Many studies report on the sintering behavior,

application of sintering additives, microstructure formation, permeability, and DC-bias superposition behavior.^[18–20] A common feature of most of the low-firing NiCuZn ferrites is their Fe deficiency, i.e., less than 50 mol% of Fe₂O₃ in the starting oxide raw materials mixture, which results in compositions of the spinel ferrites typically with less than two iron per formula unit, i.e., Me_{1.002}Fe_{1.998}O_{3.99} (instead of MeFe₂O₄ as for a regular spinel ferrite). This Fe deficiency *z*, for example, in Ni_{0.30}Cu_{0.20}Zn_{0.50+z}Fe_{2-z}O_{4-(z/2)} ferrites, provides shrinkage at low temperature and allows for sintering at 900 °C. Moreover, formation of tenorite CuO at triple points or grain boundaries during sintering at 900 °C was identified as an internal sintering aid.^[21,22]

The integration of inductive ferrite multilayer components in LTCC multilayer modules is desirable to enable further miniaturization and higher integration density.^[23,24] To successfully cofire ferrite layers and commercial LTCC tapes, the mismatch in shrinkage and thermal expansion behavior of both materials should be minimized; moreover, compatibility of both material chemistries is another important prerequisite.^[25] Taking into account all these requirements, cofiring of Ni–Cu–Zn ferrites with LTCC tapes and the fabrication of LTCC modules with integrated ferrite multilayer structures remain challenging.

1.3. Ontologies in Material Research

Applied ontologies are defined to formally model the structure of a system of interest and serve a dedicated purpose, e.g., quick search in large data sets, bridge gaps between separated data sources, etc.^[26] This contrasts to philosophical descriptions that rather aim at describing a certain reality per se without considering a dedicated background or following a direct purpose. The discipline of engineering and material science suffers from distributed data repositories, lacking reuse of already discovered insight and semantic content for informed decision-making.^[27] To overcome these shortcomings, the material community launched different research activities such as MaterialDigital with the Platform MaterialDigital core ontology (PMDco), European Materials and Modeling Ontology (EMMO), or Material Development Ontology.^[28,29] The general target of these initiatives is to accompany the material research and development process and to structure data in a reusable manner. These ontologies offer general concepts of material research and development. Therefore, the description of domain-specific insight, such as ceramic multilayer technology, requires additional descriptions. The targets of the domain ontology in this study are first to collect material, as well as production process parameters in the realm of ceramic multilayer component development; second to provide access to this data to any authorized user; and third to enable predictive simulation based on the data. A strength of the PMDco is the connection between processes such as practical tests in laboratories and documented results from these tests. With these PMDco entities, executable and sequential approaches might be well described.

The development of ontologies is becoming widespread, as it supports the rapidly increasing relevance of findable, accessible, interoperable, and reusable (FAIR) principles and open data for science. FAIR principles are driven by the urgent need to ensure

the quality of data, guarantee its reusability, and promote the advancement of scientific knowledge. Applying the FAIR principles is proving essential to manage data ethically and responsibly, and to ensure that data can be used fairly, transparently, and securely.^[30]

In today's scientific landscape, there are a variety of initiatives dealing with the FAIR principles, similar to FAIRMat.^[31] These initiatives span different disciplines and industries and have the common goal of improving the quality and reusability of data. By developing standards, guidelines, and tools, they help to ensure that data is organized and made available in a way that complies with the FAIR principles. Examples of such initiatives are FAIR data principles, GO FAIR, FAIRsharing, and FAIRplus.^[32] These efforts reflect the growing consensus in the scientific community that adherence to the FAIR principles is essential to fully realize the value of data and accelerate the advancement of scientific knowledge.

2. Results and Discussion

2.1. Material Development and Simulation

The fabrication process of LTCC modules with integrated ferrite multilayer inductors is shown in **Figure 1**. The process consists of three major parts: 1) ferrite powder preparation; 2) tape casting; and 3) multilayer LTCC processing. For complete digital reproduction of the whole process chain, data were collected for every single step of the whole process chain.

In this study, this entire process chain was used to fabricate integrated multilayer inductors with five different powders of NiCuZn ferrite with different particle sizes. Five powders of Ni_{0.3}Cu_{0.2}Zn_{0.52}Fe_{1.98}O_{3.99} were synthesized by milling of the calcined raw materials resulting in powders with mean particle size (*d*₅₀) of 0.5, 0.6, 0.7, 0.8, and 0.9 μm, respectively. To investigate the effect of the process steps on sintering behavior and resulting magnetic permeability of these powder variants, ring core specimens were produced from dry-pressed powder, laminated ferrite green tapes, and co-laminates of ferrite tapes embedded between dielectric LTCC tape (CT708). To limit the experimental parameters to particle size and manufacturing depth, all samples and prototypes were fired under nominally identical conditions (4 h at 900 °C in air). **Figure 2a** shows a scanning electron microscope (SEM) micrograph of the 0.5 μm powder. A selection of sintered specimens is presented in **Figure 2b**, with the LTCC material CT708 with blue color and the ferrite. Dense microstructures are achieved for dry-pressed samples and co-laminated samples by firing at 900 °C. **Figure 2c** shows the sintered microstructure of a pressed and sintered 0.5 μm powder sample with a relative density of 97.9% and a mean grain size of 1.1 μm. In **Figure 2d**, the cross section of a cofired co-laminate is presented, showing a dense microstructure and defect-free interfaces. However, close examination of SEM micrographs reveals a 3–5 μm thick interface layer in the ferrite. This layer is infiltrated by the LTCC glassy phase during sintering and thus exhibits increased densification and different composition.

The sintered ferrite bulk samples exhibit an increase of density after sintering at 900 °C with decreasing powder particle size. Ferrite powder with *d*₅₀ = 0.9 μm results in a relative sintered

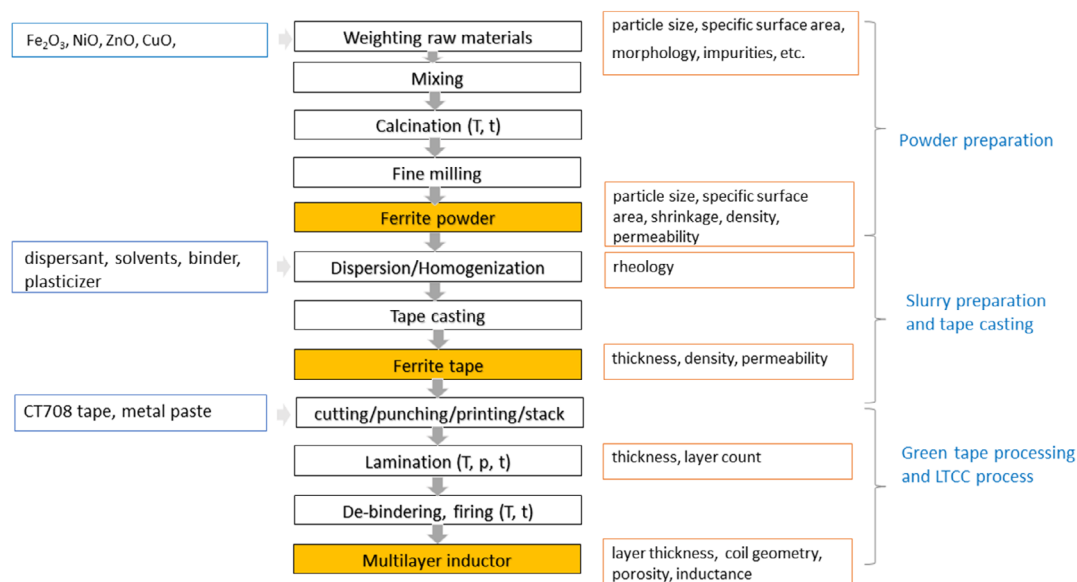


Figure 1. Scheme of process chain for the fabrication of integrated ferrite multilayer inductors; process steps with technical parameter data (middle); raw materials (left); and measured property data (right).

density of 84%, whereas powder with $d_{50} = 0.5 \mu\text{m}$ results in a sintered density of 98%. This is due to a higher sintering activity of the fine-milled powder as compared to a coarse powder and is reflected in a stronger shrinkage of the fine-milled powder measured using dilatometry (not shown here). Accordingly, the relative permeability of dry-pressed samples made from coarse powder with $d_{50} = 0.9 \mu\text{m}$ is $\mu_r = 140$, whereas that of a dry-pressed ring core made from fine-milled powder with $d_{50} = 0.5 \mu\text{m}$ shows a higher permeability of $\mu_r = 380$ (Figure 3a). Generally, the permeability scales with density and grain size.^[33] Since the bulk samples show a very small increase of grain size from $g = 0.95 \mu\text{m}$ for powder particle size of $d_{50} = 0.9 \mu\text{m}$ to $g = 1.14 \mu\text{m}$ for powder particle size of $d_{50} = 0.5 \mu\text{m}$, the permeability in that range of grain sizes shows an almost linear dependency on density.

The permeability of sintered ferrite tape laminates follows the same trend. Although, laminated samples produced from powder with $d_{50} = 0.7 \mu\text{m}$ and smaller exhibit smaller permeability than their dry-pressed counterparts. These differences cannot be attributed to density. The corresponding densities of pressed and laminated samples differ only slightly. However, the differences in fabrication technology and sample thickness apparently result in a reduction of magnetic permeability of multilayer samples, especially with regards to these finer powders that result in relative densities above 90%.

Regarding integrated multilayer inductors, the influences of cofiring must also be considered. These can be observed on the co-laminated samples. Figure 3a shows that the permeability of co-laminated and cofired samples is significantly lower as compared to bulk ferrite samples. For the $0.6 \mu\text{m}$ powder, for example, the permeability is ranked as follows according to processing technology: $\mu_r, \text{dry pressed} = 362 > \mu_r, \text{laminate} = 178 > \mu_r, \text{co-laminate} = 77$. The permeability in the cofired multilayer is reduced by 79% as compared to a bulk sample. The main reason

for this is the lower density of the embedded ferrite layers due to constrained sintering effects during cofiring with the LTCC tape layers.

However, we successfully cofired integrated multilayer inductors with ferrite layers sandwiched between LTCC layers. For the fabrication of integrated ferrite multilayer inductors, the CT708 and ferrite tapes were cut, and VIAs were punched and filled with AgPd VIA fill paste. Spiral coil patterns on the ferrite tape and contact pads on the CT708 tapes were screen-printed using a AgPd paste. Finally, multilayers as shown in Figure 2e were stacked, laminated, and cofired at 900°C . In any case, CT708 serves as top and bottom layer. Ferrite tapes with different powder particle sizes (designated 0.9–0.5) are used as inner layers. Reference samples (designated CT) with CT708 as inner layers were also prepared. The coil pattern was printed on the top side of the lower inner ferrite layer. As an example, an X-ray radiography image of a cofired integrated ferrite multilayer inductor with 10 windings is shown in Figure 2f.

The inductance of the multilayer inductors is plotted in Figure 3b. In principle, a high permeability of the ferrite layer leads to a higher inductance of the inductor component. The effect of embedded ferrite is clearly visible when comparing inductors with embedded ferrite layers (samples 0.9–0.5) with the reference without ferrite layers (CT). The multilayer ferrite inductors exhibit inductances from $L = 1.5 \mu\text{H}$ to $L = 2.1 \mu\text{H}$, whereas the reference multilayer inductor shows $L = 0.4 \mu\text{H}$ only. The integrated multilayer ferrite inductors show a correlation between powder particle size and inductance. This observation is in accordance with the expectations based on the permeabilities of the co-laminates.

The results shown here demonstrate that the concept of a cofired integrated multilayer inductor with NiCuZn–ferrite layers embedded in an LTCC multilayer arrangement is fundamentally effective and technically feasible. Nevertheless, the

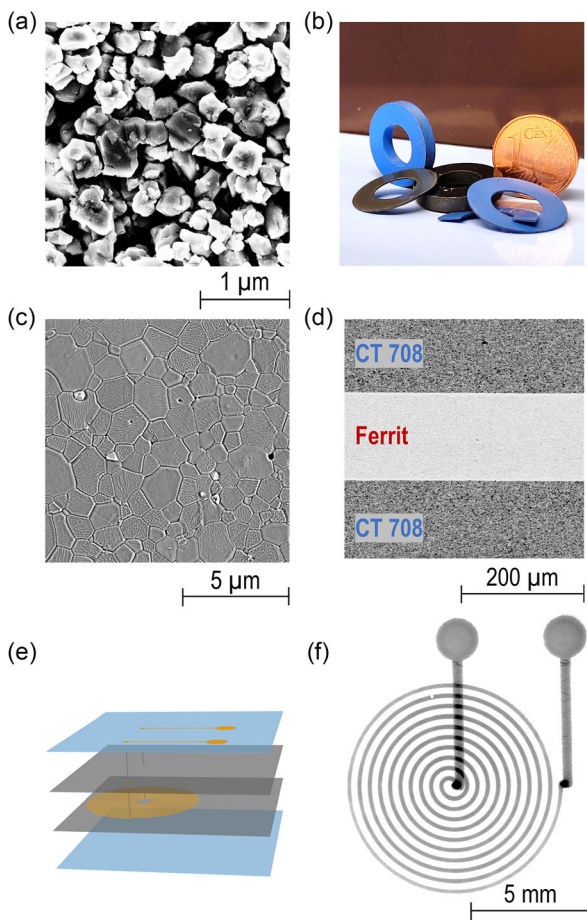


Figure 2. Micro- and photographs illustrating different steps in the fabrication of integrated ferrite multilayer inductor: a) SEM micrograph of milled ferrite powder with $d_{50} = 0.5 \mu\text{m}$; b) photograph of sintered ferrite ring cores for the measurement of magnetic permeability, pressed and sintered ferrite (middle), sintered multilayer ferrite (lower left), cofired LTCC/ferrite multilayer (lower right); c) SEM micrograph of sintered ferrite microstructure; d) SEM micrograph of cross section of LTCC/ferrite cofired multilayer; e) design of integrated ferrite multilayer inductor; and f) X-ray radiography image (top view) of printed spiral coil inside a cofired LTCC/ferrite multilayer inductor.

many parameters of the manufacturing technology significantly affect the performance of the multilayer components, which must be considered in the component design. Using proper material parameters is crucial for reliable component simulation for design development. This is illustrated by the simulation results in Figure 3b. The simulated inductance of the reference (CT) is fairly accurate, indicating the suitability of the model. The inductance of the LTCC-integrated ferrite multilayer inductors was simulated using different datasets for the permeability of the ferrite layers. If permeability data are acquired on sintered ferrite (bulk) laminates, the resulting inductance of the multilayer component is overestimated by a factor 2–3 (red circles in Figure 3b). If, in contrast, the adequate ferrite permeability data of cofired LTCC–ferrite co-laminates is used, the simulated inductance is only slightly overestimated (blue triangles in

Figure 3b). In the reverse direction, simulation of the permeability of the ferrite layer from the measured inductance of the multilayer device gives permeabilities, which are slightly lower compared to those measured on cofired co-laminate samples (green, upside-down triangles in Figure 3a). Apparently, the permeability of the ferrite layer in the inductor prototype is lower than expected. Presumably, this is due to interactions of the ferrite layers with the metallization, which are subject of further investigations.

The reported results on the fabrication of ferrite multilayer inductors integrated in between LTCC layers allow to conclude that the individual process steps of the multilayer technology, from powder synthesis to cofiring, have complex effects on the permeability of NiCuZn ferrite layers. If these factors are properly taken into account, component properties and performance can be predicted quite reliably.

To enable successful component design, the results presented here should be considered properly. To benefit from the findings, the obtained research data should be available in a comprehensible manner. The following sections explain how this was achieved in this study.

2.2. Ontology

When developing an applicable domain ontology, the extension of one or more existing high-level ontologies provides the opportunity to reuse knowledge that has already been modeled. However, adapting it to the specific requirements of a certain domain can present a certain challenge, as the way in which the knowledge is represented has a direct influence on which methods can be used effectively. The ontology developed in this study (KN ontology, for KnowNow ontology, referring to the name of the research project) is designed based on the PMDco and has been carefully adapted to the PROV Ontology (PROV-O) standard.^[34] Furthermore, it was developed in close alignment with the concept of the EMMO ontology. This means that the upper concept and entities of PMDco served as the starting point, the KN ontology entities, concepts, and content linked to it (Figure 4).

The KN ontology comprises a hierarchical structure of terms representing the various entities, processes, and functions involved in the development of multilayer ceramic components. This structure has been developed taking into account expert knowledge and expertise to provide a precise and comprehensive representation of the development of multilayer ceramic components.

Figure 4 shows an excerpt of the KN ontology exemplarily demonstrating how the relation between permeability and density is represented. The upper part of Figure 4 shows so-called T-box statements, which are definitions of classes, categories, and relations. The bottom part shows the so-called A-box, describing specific entities, i.e., instances related to the classes they belong to, and their relations. The blue balloons represent classes which were taken from the PMDco. From these, more specific classes such as density and powder were derived for the domain ontology (shown as green balloons). From a ceramics point of view, a powder with a distinct composition and particle size distribution is considered to be an EngineeredMaterial. As

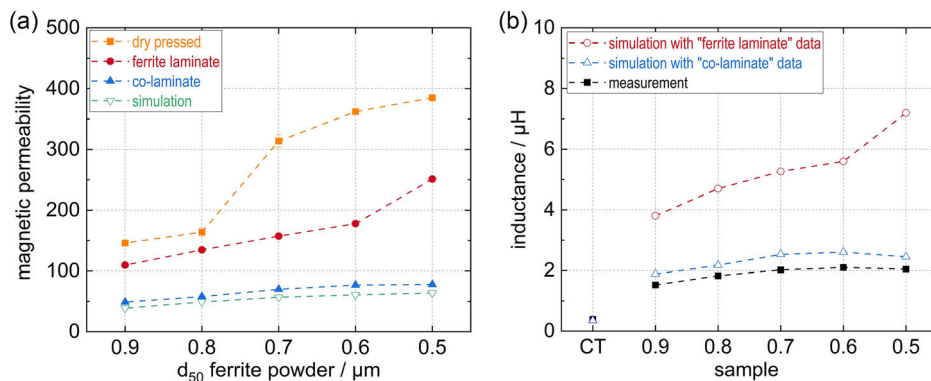


Figure 3. a) Magnetic permeability of sintered ferrite samples prepared from powders with decreasing particle size by dry pressing, lamination of ferrite tapes, and co-lamination of ferrite and LTCC tapes, and permeabilities obtained from simulation and measured inductance of cofired inductors, and b) measured inductance of cofired multilayer inductors (sample designates the material of the two inner layers), and simulated values based on ferrite permeability measured in ferrite laminates or ferrite—LTCC co-laminates.

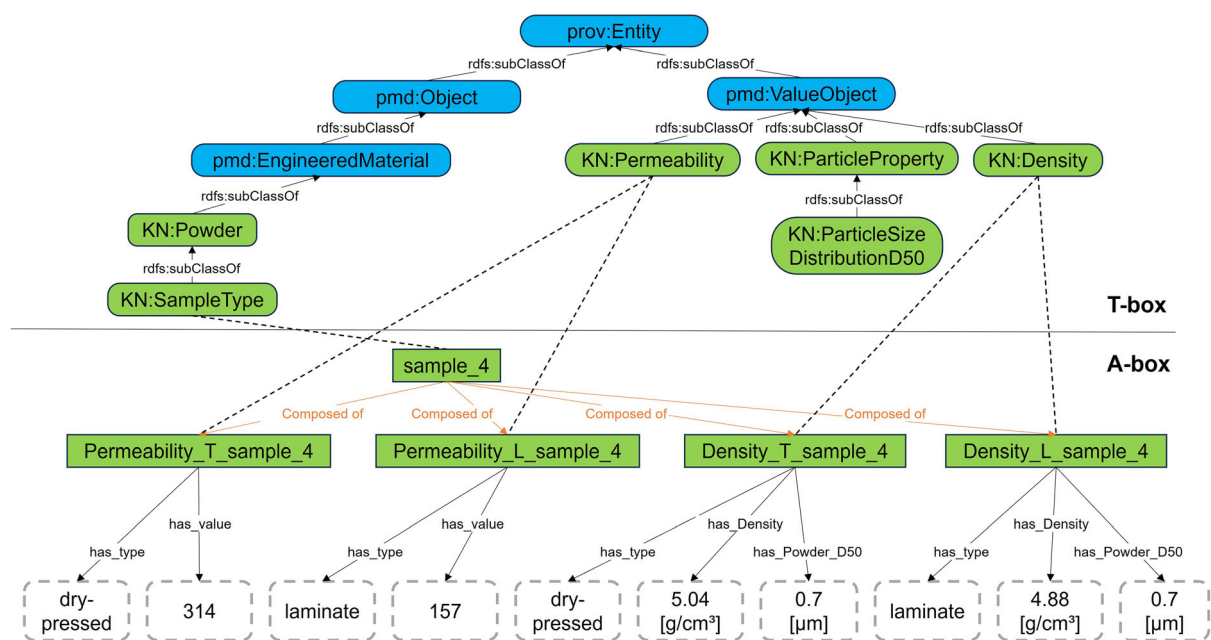


Figure 4. Excerpt of ontology-based data structure; blue boxes depict PMDco entities; green round-shaped boxes depict KN entities; green angularly shaped boxes depict KN instances; and transparent boxes depict KN value objects.

different types of samples can be produced from it, SampleType is modeled as a subclass of powder. An instance of SampleType, i.e., a dry-pressed specimen, has different properties, which are described by composed_of relations to different subclasses of ValueObject.

In the example, we consider a NiCuZn ferrite powder with a mean particle size of $d_{50} = 0.7 \mu\text{m}$ (designated sample 4). From this powder, a dry-pressed and a laminated specimen were produced and characterized. Permeability and density were measured. Structuring the respective data according to the KN ontology results in the entities shown at the bottom of Figure 4. Following the different relations, it becomes clear that a dry-pressed specimen of the respective powder has a density of 5.04 g cm^{-3} and a permeability of 314, whereas a laminated

specimen of the same powder has a density of 4.88 g cm^{-3} and a permeability of 157.

Being able to make such conclusions just from the data is especially useful if we imagine that the different measurements were performed by different groups with a large time interval at different locations. To structure independently collected data reliably and efficiently in this way, the use of automated processing procedures, so-called data pipelines, is recommended.

2.3. Data Pipeline

To conveniently and reliably acquire and structure the data collected during the study, an automated data pipeline was

implemented. The data pipeline takes conventional, unlinked research data from various sources, converts it into more processable data formats and links the included information semantically according to a domain ontology. The upload pipeline is based on the idea of minimizing the learning curve for laboratory staff. Therefore, the data conversion process is covered behind a web front end that serves as user interface. It is executed from the server and provides access to the ontology and all functionalities around it to those possessing the URL. Imperative in this setting is a backend support that runs the server as well as the user interface application. The user interface attains user commands and transfers the input and data to the corresponding functions and vice versa provides system feedback to the user. Next to the upload pipeline, a download functionality supports SPARQL (recursive acronym for SPARQL protocol and RDF query language) queries to access data stored in the ontology in a table format visualization. The upload functionality is supported with folders for different groups of researchers producing data, e.g., from different institutions. This helps users to intuitively apply the framework and provides order to the data pipelining process. After the data is successfully uploaded, confirmation is given to the user.

The upload data pipeline involves the following steps. First, different types of raw data are uploaded to a local server via a web front end and converted into a format that can be processed by machines. To link the uploaded data to a specific area of the knowledge domain, semantic triples are generated according to the Resource Description Framework (RDF) data model. An RDF triple corresponds to the form subject–predicate–object, for example, sample-has_property-density. The semantic links described in the triples correspond to the relationships defined in the ontology. Finally, this linked data is stored in a triple store database to make it accessible for logical inference using SPARQL. The pipeline is divided into four main phases: data storage, preprocessing (wrapping), mapping, and querying (Figure 5). In summary, the data pipeline takes unstructured, unrelated data from various spreadsheets as input. The wrapper converts these data to structured, unrelated data in a JavaScript Object Notation (JSON) file. In the mapping process, data from the JSON file is converted to structured and related data according to a Turtle file and stored as triples in an Web Ontology Language (OWL) file in a triple store. Data in the triple store can be explored using SPARQL queries.

The following sections describe the design rational and implemented structure of the three main steps. It should be noted that, like the structure of an ontology, there are many possibilities to design a functional data pipeline. The concepts described here generally follow the recommendations of the PMD, but, in detail, are individual solutions that were chosen with regard to the type of data and the preferences of the researchers involved.

2.3.1. Data Storage

Automated converting and linking data into the ontology requires a machine readable and reproducible structure of both the location of data as well as their inner order. This rigorous data management approach has been agreed between the involved researchers. A folder dedicated to each group in an explorer-like hierarchical directory structure predefines the storage location. The files are grouped in directories depending on the method or process, e.g., density measurements or tape-casting protocols. The individual data files uploaded to dedicated folders are expected in certain format and inner structure, e.g., a density value is expected in a designated cell.

2.3.2. Preprocessing

During the first step of the preprocessing, individual Jupyter notebooks—so-called wrappers—extract data from the various spreadsheets and transform it to a uniform data format. Such a wrapper enables a standardized data provision by means of minimal adjustments for each spreadsheet template to account for differences in parameter labels, cell positions, and sheet names. The Jupyter notebooks read, e.g., Excel files as input and generate entries in a JSON file as output. Each notebook in the framework creates its own JSON output file for a specific process or measurement method. In the preparation process, the JSON files are passed between the notebooks to seamlessly load and build on data. The use of the JSON format allows for easy data transfer and processing, optimizing the efficiency of the automated processes. Finally, a single JSON file is created that contains a structured dictionary with relevant information from the Excel files for all processes. The wrappers are triggered from the data upload without manual interference, and as a result, the global JSON file continuously grows with the uploaded data.

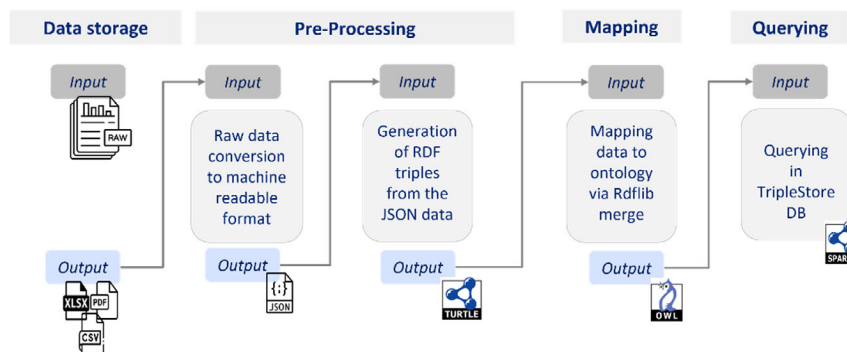


Figure 5. Data pipeline with input and output formats of each phase; data-storage, preprocessing, and mapping form the upload pipeline, querying is triggered by the user and added here for the sake of completeness.

The wrappers are established using the Python libraries Pandas and Openpyxl to simplify the handling of Excel files. Pandas enables efficient data processing, while Openpyxl specializes in the direct extraction of data from Excel files.^[35,36]

In the second step of the data preprocessing, the semantic relations between the data stored in the JSON file are described as triples. Data types, i.e., classes and entities, are considered, i.e., “density” or “milling time”, not actual values such as “2.9 g cm⁻³” or “180 min”. Triples are described in Turtle files (Terse RDF Triple Language, extension.ttl). In the preparation phase, a single Jupyter notebook is used to automatically create the required triples according to the predefined KN ontology. The Jupyter notebook allows for modular and scalable automation by splitting the code into separate cells that can be executed independently. The interactive nature of Jupyter facilitates debugging, visualization of intermediate results, and efficient iteration during development.

2.3.3. Mapping

In the mapping process, actual data is structured as triples, according to the general descriptions in the Turtle file, and stored in an OWL file. For example, a permeability measurement of $\mu_t = 314$ results in the triple “Permeability”-has_value-“314”, where “Permeability” is a class, has_value is a property, and “314” is an instance. To really describe knowledge with this approach, a multitude of interconnected triples needs to be created.

The Turtle file contains various data elements necessary for the mapping, including the following: 1) prefix definitions: defining the namespaces that will be used throughout the Turtle document to simplify the representation of URIs (uniform resource identifiers); 2) new class and property definitions: this creates new classes and properties that were not previously present in the main ontology, for example, the class “Permeability” with the property “has_value”; 3) instances of classes: each instance represents a specific material property or process and is linked to the corresponding class via RDF:type statements; and 4) triples for linking data: the RDF triples are automatically generated to establish relationships between instances, properties, and classes. This enables the hierarchy and links in the input data to be recorded precisely.

The hierarchy of RDF triples divides the data structure into different levels to capture complex relationships between the data. These include the following: 1) Level 0 triples: these establish the most important link between the main data set and, for example, the individual worksheets of an Excel file; 2) Level 1 triples: these indicate the relations between worksheets and the associated process or property instances; 3) Level 2 triples: these record the connections between the instances and their data attributes by linking properties to their values; and 4) Level 3 triples: links are deepened here by representing specific instances and their nested properties.

The data mapping automation is facilitated by the use of Jupyter Notebook and RDFLib.^[37] The focus here is on converting JSON data into RDF triples and storing them in an OWL file. RDFLib enables the automatic generation of classes, data attributes, and object properties from the structured JSON data. This

also includes linking instances of classes with the corresponding attributes and values. In addition, the system automatically reads the JSON file, converts it into a Python dictionary, and processes it to create the RDF graph. Namespaces are initialized correctly and triples are added systematically.

The integration of the newly assigned data into the domain ontology is automated by Apache Jena Fuseki, an open source semantic web framework that can be run as server to handle RDF data.^[38] Data from a new Turtle file is combined with the existing domain ontology to extend the RDF dataset. Apache Jena Fuseki Server automatically recognizes the instances from the new file and links them to the corresponding classes and properties in the main ontology. This eliminates the need to redefine elements in the new file, enabling efficient and accurate integration.

2.4. Usage Demonstration

2.4.1. Data Upload

The data pipeline is streamlined and requires a lab technician to enter data to start the automated data pipeline. With this approach, researchers are relieved from the burden of programming tasks, as the process relies solely on drag-and-drop functionality. In addition, the system is designed for versatility so that it can easily be used by other users for other applications.

Figure 6a shows a screenshot of the web front end. Clicking the “Choose File”-button opens a common open-file dialogue to select the files intended for upload. Folder selection by the radio button helps to presort the data for accurate storage. Here, each of the involved research institutes has a dedicated folder. These folders are automatically scanned for new data, e.g., once a day. If new data is detected, the execution of the data pipeline is triggered automatically.

2.4.2. Data Retrieval

Users can access the data from the triple store by means of SPARQL queries. Certainly, the formulation of SPARQL queries is rather impractical for untrained users. Thus, the direct entry of queries should be understood as interim solution. Further development is foreseen to implement natural language processing to simplify the creation of SPARQL search strings. However, to demonstrate data retrieval, Figure 6b shows the syntax of an SPARQL query that asks for all available permeability data of a given powder sample (sample_4_052021) and the related data objects. This represents the use case of a component designer exploring the data and trying to understand why different results are obtained with the same material.

The output is given in Figure 6c. It shows a table with three different permeability values in the column “Permeability_value”. Closer examination teaches the user two important things: first, there are three different types of samples (blue arrows in Figure 6c: dry pressed, laminate, co-laminate); second, each sample type is related to a different density value (highlighted in yellow in Figure 6c). This informs the nonexpert that the type of manufacturing has an influence on the achievable density and magnetic properties. Hence, the nonexpert is able to

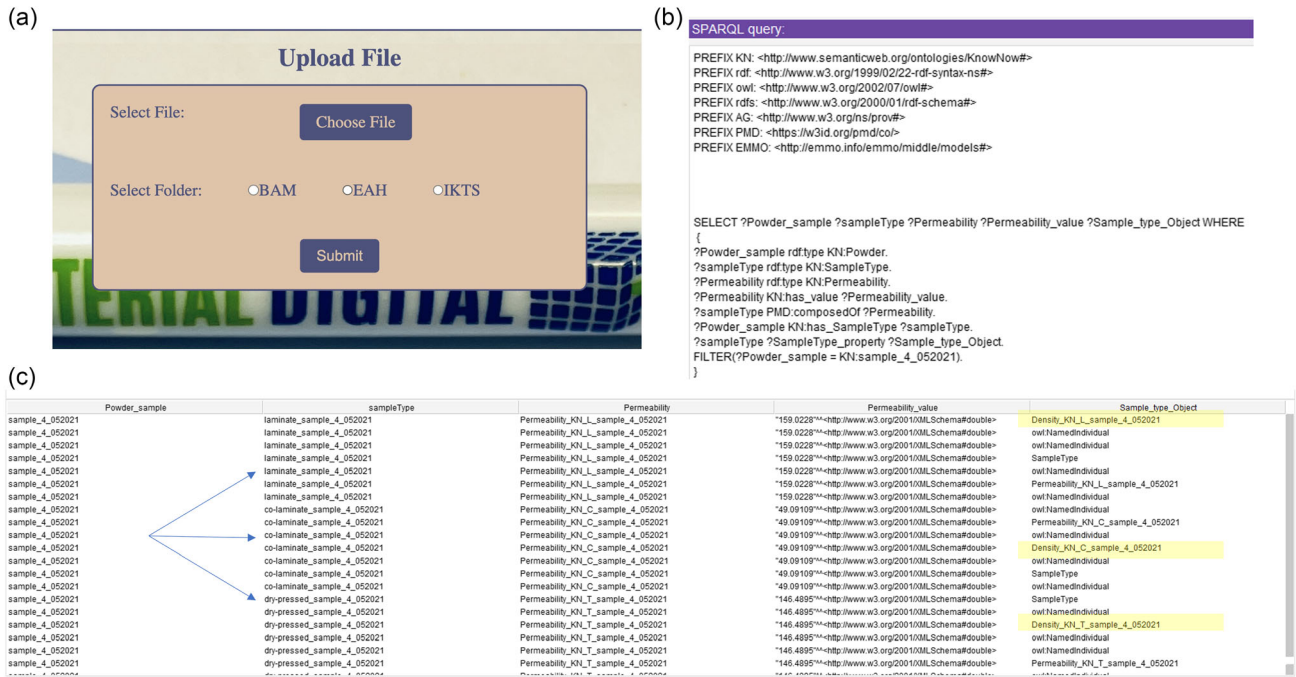


Figure 6. a) User interface of the web front end to upload data, b) example of an SPARQL query to retrieve data from the triple store, and c) output of the example query.

select the correct data for a component simulation, for example, without necessarily having to consult a domain expert.

3. Conclusion

This study demonstrates the integration of NiCuZn ferrite as magnetically active material in a cofired ceramic multilayer inductor. The inductance of the prototype is increased by the factor of five compared to a similar multilayer inductor without integrated ferrite (2.1 μH compared to 0.4 μH). However, the multilayer manufacturing process affects the magnetic permeability of the ferrite, resulting in decreased permeability of cofired tape co-laminates compared to dry-pressed samples. Predictive simulation of prototype inductance necessitates the selection of appropriate permeability data. An automated data pipeline is introduced to convert the conventionally acquired, unstructured, and unlinked process and material data to machine-readable and semantically linked data. In this way, the relevant influencing variables and effects (here, e.g., sample type and permeability) can also be understood by nonexperts using the available data retrieved by an SPARQL query. This enables component designers, for example, to select suitable input data for simulations.

The data pipeline presented shows how conventionally collected data can be stored in a FAIR and semantically linked manner with practically no additional effort for technical or scientific personnel. It is also a practical application example of the concept pursued by the initiative Platform Material Digital (PMD) to create a material data space.

4. Experimental Section

Material Development: For powder synthesis, the raw materials Fe_2O_3 (Voest Alpine), NiO (Lohmberg), CuO (Alfa Aesar), and ZnO (Tridelta) were weighed in stoichiometric amounts and mixed for 24 h in deionized water in a ball mill (100 rpm, 3 mm ZrO_2 milling beads). The mixture was dried (12 h, 95 °C), sieved (630 μm mesh), and calcined (2 h, 850 °C). Five different ferrite powders with mean particle sizes d_{50} of 0.9, 0.8, 0.7, 0.6, and 0.5 μm were obtained by milling (planetary ball mill, 170 rpm, 1 mm ZrO_2 milling beads, deionized water) for 0.5, 0.75, 1.25, 2, and 4 h, respectively. Particle size distributions were measured by laser diffraction (Malvern Mastersizer 2000).

For tape casting, ferrite powders were mixed with methyl ethyl ketone mixture (MEK/EK) as solvent and dispersants and mixed for 24 h. After addition of binders and plasticizers, the slurry was homogenized for another 24 h. After evaluation of the slurry rheology, ferrite tapes with thickness of 200 μm were fabricated using a doctor-blade tape-casting machine. A lead-free, commercially available LTCC tape (CT 708) was used for co-laminates and multilayer inductors.

Ring core specimens were prepared from calcined powder by dry pressing. Laminate and co-laminate specimens were prepared by uniaxial lamination (thermoccompression, 80 °C, 24 MPa) of green tapes (6 layers ferrite, or 2/2/2 layers CT708/ferrite/CT708, respectively) and manually punching of the core.

The multilayer conductors were fabricated by punching and filing the VIAs (200 μm , Ag/Pd paste Dupont DP 6138), screen printing of coil patterns and contact pads (Ag/Pd paste Dupont 6146), and stacking and uniaxial lamination in a custom tool (80 °C, 24 MPa). The 70 × 70 mm panels were fabricated, one integrated multilayer from each ferrite tape variant and an LTCC only multilayer as reference. Each panel contained three of the coil patterns in addition to other test structures.

All specimen and multilayer were sintered at 900 °C for 4 h in air (0.5 K min^{-1} to 500 °C for debinding, further heating with 4 K min^{-1} to 900 °C). Porous SiC setters were placed on the laminates, co-laminates, and inductors to ensure flatness.

Magnetic permeability of the specimens was measured using an impedance analyzer (Agilent E4991A) and a dedicated sample holder from 1 MHz to 1000 MHz. Two dry-pressed and laminated samples and one co-laminate of each powder variant were measured. Inductance was measured using a Keysight E4990A with Keysight 16047E test fixture. Three samples were tested for each inductance data point.

Simulation: Finite-element method simulations of inductance and magnetic permeability were performed with COMSOL Multiphysics (version 6.1) using MATLAB integration. An axisymmetric 2D approximation of the coil was used, in which the coil spiral was replaced by circles with the mean radii of the individual coil windings. This spiral was embedded between two layers of ferrite and these in turn were embedded between two layers of CT708. The layers were infinite in the x/y plane. The individual thicknesses were taken from cross sections of the sintered inductor prototypes. Radiography data for the lateral measures (start radius, winding spacing, width of conductor tracks) of the coil were used for the geometry data. The entire coil package was surrounded by air and extended to infinity by an infinite-element domain for numerical reasons. A customized mesh with so-called boundary layers was used for better consideration of the skin effect. Magnetic and electric fields interface (COMSOL AC/DC module) with the RLC Coil group option was used, considering magnetic losses in the ferrite layers. The outer boundary of the simulation area was assumed to be magnetically insulating and 1 V was used as the excitation voltage of the coils. To be able to calculate the necessary comparative simulations for all measured coils in one run, the possibility of connecting MatLab and COMSOL was used. Within a MatLab script, all geometry measures were loaded and a simulation was configured sequentially for all coils with these and the corresponding material configuration, executed and the results were read out and saved in corresponding data files. All files necessary to perform these simulations, including MatLab scripts and material data, are provided as Supporting Information.

Implementation Details: The server was a university-hosted local server that features sufficient memory and calculation capacities for the project purpose as well as web access and secure data hosting behind a firewall. Windows and Unix served as applicable operating systems, regular personal computer calculation power was sufficient for the operation of the pipeline, internet connection was not required.

The user interface was implemented with Python language, as IDE Jupiter Notebook was used. The commented code is available as Supporting Information.

The open-source ontology editor Protégé (protege.stanford.edu) was used to develop the KN.

Acknowledgements

The authors thank the German Federal Ministry of Education and Research (BMBF) for the financial support of the project "KNOW-NOW" through project funding FKZ 13XP5123A-D. Felipe Baca, Simplicio Guejipe Dowouo, and Anton Dybov supported the TU Berlin programming work. Manuela Heymann (IKTS) and Peter Krüger (IKTS) are acknowledged for providing radiography images of the prototypes.

Open Access funding enabled and organized by Projekt DEAL.

Conflict of Interest

The authors declare no conflict of interest.

Data Availability Statement

The data that support the findings of this study are openly available in DepositOnce at <https://doi.org/10.14279/depositonce-20150>, reference number 20150; <https://doi.org/10.14279/depositonce-20387>, reference number 20387; and <https://doi.org/10.14279/depositonce-20352>, reference number 20352.

Keywords

ceramics, multilayer inductors, ontologies

Received: April 30, 2024

Revised: June 14, 2024

Published online:

- [1] B. Bayerlein, T. Hanke, T. Muth, J. Riedel, M. Schilling, C. Schweizer, B. Skrotzki, A. Todor, B. Moreno Torres, J. F. Unger, C. Völker, J. Olbricht, *Adv. Eng. Mater.* **2022**, *24*, 2101176.
- [2] A. Valdestilhas, B. Bayerlein, B. Moreno Torres, G. A. J. Zia, T. Muth, *Adv. Intell. Syst.* **2023**, *5*, 2300051.
- [3] J. Kimmig, S. Zechel, U. S. Schubert, *Adv. Mater.* **2021**, *33*, 2004940.
- [4] L. Himanen, A. Geurts, A. S. Foster, P. Rinke, *Adv. Sci.* **2019**, *6*, 1900808.
- [5] B. G. Pelkie, L. D. Pozzo, *Digital Discovery* **2023**, *2*, 544.
- [6] K. Hong, T. H. Lee, J. M. Suh, S.-H. Yoon, H. W. Jang, *J. Mater. Chem. C* **2019**, *7*, 9782.
- [7] S. Mohith, A. R. Upadhya, K. P. Navin, S. M. Kulkarni, M. Rao, *Smart Mater. Struct.* **2020**, *30*, 013002.
- [8] D. Jurków, T. Maeder, A. Dąbrowski, M. S. Zarnik, D. Belavič, H. Bartsch, J. Müller, *Sens. Actuators, A* **2015**, *233*, 125.
- [9] Y. Imanaka, *Multilayered Low Temperature Cofired Ceramics (LTCC) Technology*, Springer, New York **2004**.
- [10] L. Ren, X. Luo, H. Zhou, *J. Am. Ceram. Soc.* **2018**, *101*, 3874.
- [11] T. Reimann, S. Barth, B. Capraro, H. Bartsch, J. Töpfer, *Ceram. Int.* **2021**, *47*, 27849.
- [12] R. N. Basu, F. Tietz, E. Wessel, D. Stöver, *J. Mater. Process. Technol.* **2004**, *147*, 85.
- [13] H. Naghib Zadeh, G. Oder, J. Hesse, T. Reimann, J. Töpfer, T. Rabe, *J. Electroceram.* **2016**, *37*, 100.
- [14] B. Brandt, H. Naghib-Zadeh, T. Rabe, J. Blendell, *J. Am. Ceram. Soc.* **2013**, *96*, 726.
- [15] P. Guzdek, J. Kulawik, K. Zaraska, A. Bieńkowski, *J. Magn. Magn. Mater.* **2010**, *322*, 2897.
- [16] A. Nakano, T. Nomura, *Encyclopedia of Materials: Science and Technology*, Elsevier **2001**, pp. 5859–5863, <https://doi.org/10.1016/B0-08-043152-6/01020-2>.
- [17] H.-I. Hsiang, *J. Mater. Sci.: Mater. Electron.* **2020**, *31*, 16089.
- [18] J. Mürbe, J. Töpfer, *J. Electroceram.* **2006**, *16*, 199.
- [19] H.-I. Hsiang, J.-F. Chueh, *Int. J. Appl. Ceram. Technol.* **2015**, *12*, 1008.
- [20] Y. Wang, Y. Jing, S. Che, Y. Li, Z. Xu, X. Tang, *J. Electron. Mater.* **2020**, *49*, 3325.
- [21] H. Su, X. Tang, H. Zhang, L. Jia, Z. Zhong, *J. Magn. Magn. Mater.* **2010**, *322*, 1779.
- [22] J. Mürbe, J. Töpfer, *J. Magn. Magn. Mater.* **2012**, *324*, 578.
- [23] R.-T. Hsu, J.-H. Jean, Y.-Y. Hung, *J. Am. Ceram. Soc.* **2008**, *91*, 2051.
- [24] C. Glitzky, T. Rabe, M. Eberstein, W. A. Schiller, J. Töpfer, S. Barth, A. Kipka, *J. Microelectron. Electron. Packag.* **2009**, *6*, 49.
- [25] T. Rabe, H. Naghib-Zadeh, C. Glitzky, J. Töpfer, *Int. J. Appl. Ceram. Technol.* **2012**, *9*, 18.
- [26] N. Guarino, D. Oberle, S. Staab, *Handbook on Ontologies*, Springer, New York **2009**, pp. 1–17, https://doi.org/10.1007/978-3-540-92673-3_0.
- [27] Gogineni S., Exner K., Stark R., Nickel J., Oeler M., and Witte H. in *Metadata and Semantic Research: 13th Int. Conf., MTSR 2019*, Springer, Rome, Italy, October **2019**, Revised Selected Papers, **2019**.
- [28] H. Li, R. Armiento, P. Lambrix, *The Semantic Web – ISWC 2020*, Springer International Publishing, Cham **2020**.
- [29] B. Bayerlein, M. Schilling, H. Birkholz, M. Jung, J. Waitelonis, L. Mädler, H. Sack, *Mater. Des.* **2024**, *237*, 112603.

- [30] M. D. Wilkinson, M. Dumontier, I. J. Aalbersberg, G. Appleton, M. Axton, A. Baak, N. Blomberg, J.-W. Boiten, L. B. Da Silva Santos, P. E. Bourne, J. Bouwman, A. J. Brookes, T. Clark, M. Crosas, I. Dillo, O. Dumon, S. Edmunds, C. T. Evelo, R. Finkers, A. Gonzalez-Beltran, A. J. G. Gray, P. Groth, C. Goble, J. S. Grethe, J. Heringa, P. A. C. 'T Hoen, R. Hooft, T. Kuhn, R. Kok, J. Kok, et al., *Sci. Data* **2016**, 3, 160018.
- [31] A. E. Mansour, L. Rotheray, K. Helbig, S. Botti, H. B. Weber, M. Aeschlimann, C. Draxl, in *Proc. Conf. Research Data Infrastructure*, September **2023**.
- [32] A. Jacobsen, R. De Miranda Azevedo, N. Juty, D. Batista, S. Coles, R. Cornet, M. Courtot, M. Crosas, M. Dumontier, C. T. Evelo, C. Goble, G. Guizzardi, K. K. Hansen, A. Hasnain, K. Hettne, J. Heringa, R. W. W. Hooft, M. Imming, K. G. Jeffery, R. Kaliyaperumal, M. G. Kersloot, C. R. Kirkpatrick, T. Kuhn, I. Labastida, B. Magagna, P. Mcquilton, N. Meyers, A. Montesanti, M. Van Reisen, P. Rocca-Serra, et al., *Data Intell.* **2020**, 2, 10.
- [33] C. Priebe, J. Töpfer, *J. Magn. Magn. Mater.* **2022**, 560, 169581.
- [34] T. Lebo, S. Sahoo, D. McGuinness, K. Belhajjame, J. Cheney, D. Corsar, D. Garijo, S. Soiland-Reyes, S. Zednik, J. Zhao, *W3C Recommendation*, Vol. 30, **2013**, <https://www.w3.org/TR/prov-o/> (accessed: April 2024).
- [35] Pandas - Python Data Analysis Library, <https://pandas.pydata.org/> (accessed: January 2024).
- [36] E. Gazoni, C. Clark, Openpyxl - A Python Library to Read/Write Excel 2010 xlsx/xlsm files, <https://openpyxl.readthedocs.io/en/stable/> (accessed: April 2024).
- [37] C. Boettiger, J. Ooms, K. Leinweber, J. Hester, ropensci/rdfliib: v0.2.3. 2020: Zenodo.
- [38] Apache Jena Fuseki, <https://jena.apache.org/documentation/fuseki2/> (accessed: April 2024).